Springer

KSME

Journal of Mechanical Science and Technology 28 (3) (2014) 953~961
www.springerlink.com/content/1738-494x
DOI 10.1007/s12206-013-1115-6

A cam-quadrilateral mechanism for power transmission of a twin-rotor piston engine †

Xiaojun Xu[1], Hao Deng[2,*], Cunyun Pan[1] and Haijun Xu[1]

[1]*College of Mechatronics Engineering and Automation, National University of Defense Technology, Changsha, 410073, China*
[2]*Qingdao Branch, Naval Aeronautical engineering Institute, Qingdao, 266041, China*

(Manuscript Received December 20, 2011; Revised October 16, 2013; Accepted November 6, 2013)

Abstract

A quadrilateral with four invariable lengths of sides has the characteristic of transforming the variation of the diagonal length to the variation of its interior angle. Thus, the combination of two quadrilaterals with a cam forms the differential velocity drive mechanism (DVDM) of a novel twin-rotor piston engine (TRPE). The DVDM restricts the two coaxial rotors to rotate with periodical but nonuniform velocity, and the volume of working chambers created by the adjacent vane pistons of the two rotors alternately expands and then contracts. The volumetric change of working chambers is used to generate the four-stroke engine cycle. The kinematic model and the detailed position, velocity, and acceleration analysis results of the TRPE are presented. The results show that this novel engine, associated with the advantages of higher uniformity of torque and power density due to multiple power strokes per revolution of the output shaft, has a compact and totally balanced design.

Keywords: Piston engine; Power density; Cam; Quadrilateral; Transmission

1. Introduction

The reciprocating piston engine provides the power for transport on land, sea and in the air in greater numbers than any other devices [1]. Most of the improvements on reciprocating engines have been associated with fuels [2], lubricants [3], materials [4], and most significantly, the process of getting the fuel and gases in and out of the cylinder [5-7]. But the basic internal layout of crankshaft-connecting rod-piston mechanism, which is derived from steam engine practice, has never really been challenged. In reciprocating piston engines, the pistons must stop and reverse direction four times per revolution of the output shaft in a four-stroke engine. Those engines also require rather complex valve systems. Thus, inventors from all over the world have been proposing many novel engines to reduce the inherent disadvantages of the reciprocating engine [8-11].

Efforts to develop rotary internal combustion engines also have been undertaken in the past [12], and are continuing [13-16]. One main advantage with a rotary engine is reduction of inertia loads and better dynamic balance. The Wankel engine is the most famous one which achieved a little production success [17]. It can provide one power stroke for each revolution of the output shaft. Its sealing problems, poor combustion conditions, and the complex manufacture and repair haven't been properly solved until now.

Currently, under the demands of high power density and high efficiency, the oscillatory rotating type engine [18] has gained the most rapid development. Librovich [19, 20] proposed a novel rotary vane engine which uses non-circular gears for torque transmission. Cheng [21, 22] studied the eccentric circular-noncircular gear driving system of a differential velocity pump. Liang [23] proposed a rotary engine with two rotors and its design method. Chun [24] used the half rounded gear to alternately lock and unlock the rotors of his rotary engine. Sakita [25, 26] described his cat-and-mouse type rotary engine and its performance evaluation. Mikio [27] utilized grooves and rods for power conveyance in his cat-and-mouse type rotary device. Wieslaw [28] revealed a new oscillating engine concept. Shih [29] analyzed the kinematics of the cycloidal internal combustion engine mechanism. It appears from the published literature that all these proposals have unbalanced mass and various disadvantages.

In this study, a cam-quadrilateral mechanism for power transmission on a twin-rotor piston engine (TRPE) is patented [30, 31] and introduced. Compared to available piston engines, it can provide significantly more power stroke per output shaft rotation, and has a compact and totally balanced structure. The kinematic modeling and analysis of the TRPE are discussed.

*Corresponding author. Tel.: +86 84574931, Fax.: +86 84574931
E-mail address: xuxiaojunmail@sina.com
† Recommended by Associate Editor Sung Hoon Ahn

The analysis results are presented to demonstrate the main motion characteristics of the engine.

2. Structure and work principle of the TRPE

The simplest type of the TRPE is shown in Fig. 1. The basic mechanical structure of this engine, without considering the combustion system, cooling system, and lubricating system temporarily in this paper, includes the two major assemblies, an energy conversion system (ECS) and a differential velocity drive mechanism (DVDM).

ECS has two identical opposed rotors, the former rotor and the latter rotor. The rotors are intersected mounted and enclosed in a stationary ECS housing. In operation, the two rotors are driven by an expanding ignited gas and rotate about a common axis in the same direction as indicated by arrows shown in Fig. 1(a) to convert heat energy into mechanical energy.

In general, the engine has $2N$ (N is a natural number) sectoral vane pistons in total. Vane pistons are radially attached to the rotor hub of each rotor. In a preferred embodiment as shown in Fig. 1, each rotor has four vane pistons. The vane pistons on the former rotor are designated "Y_1" to "Y_4", and the same on the latter rotor are designated "L_1" to "L_4". Vane pistons extend the full width of the housing, and these eight vane pistons divide the ECS housing into eight separate working chambers. Each of the working chambers, denoted by Ⅰ~Ⅷ, is located between a vane piston on the former rotor and its adjacent vane piston on the latter rotor. Such that at any one time, one set of four separate working chambers is close together while the other set is wide apart.

Intake and exhaust ports are provided at a fixed angular position relative to the ECS housing. In the case of the spark ignition engine with four vane pistons per rotor, See Fig. 1(a), two ignition devices (P_{ig1}, P_{ig2}), two intake ports (P_{in1}, P_{in2}), and two exhaust ports (P_{ex1}, P_{ex2}) are radially located at the circumference of the ECS housing. Each stroke commences or completes while any working chamber travels close to the ports.

DVDM interconnects the two rotors and causes them to alternately speed up and slow down at certain time. This oscillating rotary movement of the rotors is controlled by a cam-quadrilateral mechanism in this paper. The quadrilateral with four invariable lengths of sides has the characteristics of transforming the variation of the diagonal length to the variation of its interior angle. Based on this principle, and for a totally balanced structure, the preferred embodiment of a DVDM is shown in Fig. 1(b). The main part of the DVDM is the combination of two quadrilaterals with a cam. A quadrilateral is denoted by $OABC$. As the length of diagonal OB is increasing, the angle between OA and OC is also increasing respectively, and vice versa.

In particular, the DVDM consists of a stationary cam, an output stick, two rockers, two sliders, four connecting rods, and a stationary DVDM housing. The DVDM housing is co-

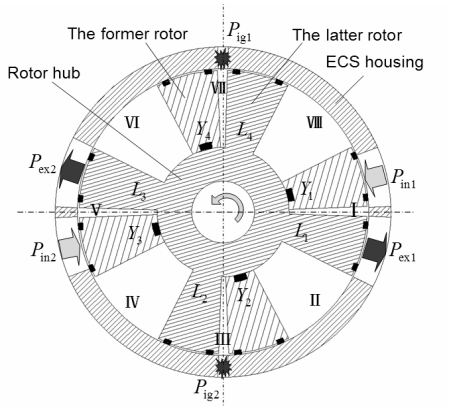

(a)

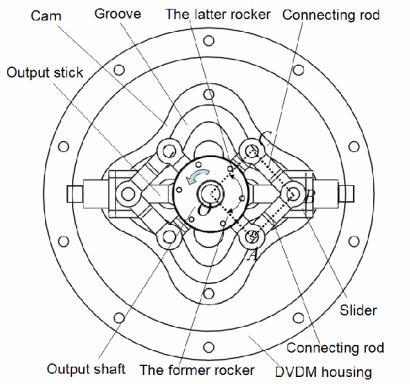

(b)

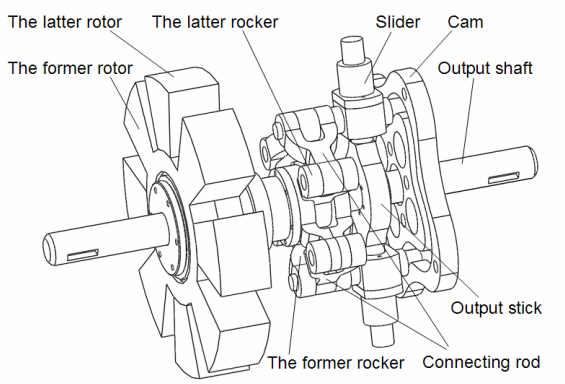

(c)

Fig. 1. Scheme of the TRPE with four vane pistons per rotor: (a) ECS; (b) DVDM; (c) assembly view of ECS and DVDM, housings are not shown.

axial with and affixed to the ECS housing. The output shaft is rigidly connected to the output stick (OB). As the output shaft rotates, the slider (B) moves constrained by the output stick (OB) and the curved groove on the cam simultaneously, i.e., it will rotate about and move toward and away from the center (O) alternately. This special motion of the slider (B) creates the periodic oscillation of the relative angular velocity between the former rocker (OC) and the latter rocker (OA). As the former rotor is rigidly connected to the former rocker, and

the latter rotor is rigidly connected to the latter rocker, the rotors are constrained to move with the same variable oscillatory rotation at a different pace. This type of relative motion between the rotors generates the volumetric change within each working chambers and creates the four−stroke cycle.

3. Mathematical modeling of the TRPE

3.1 Kinematic modeling of the TRPE

As the rockers are fixed to, and thus represent the kinematic characteristics of the respective rotors, the kinematic relationship between the output shaft and the rotors can be obtained from the kinematic model of DVDM. The initial position of TRPE and positive direction of x− and y- coordinates are defined and shown in Fig. (2); TRPE is a one degree of freedom planar mechanism. Assume the quadrilateral *OA'B'C'* is designed as the same with *OABC* for balance and strength. Thus, it is enough to analyze the motion pattern of one quadrilateral. l_1~l_4 is, respectively, the length parameters of the quadrilateral *OABC*, and all angles are measured from the *x*−axis in the counter-clockwise direction.

ρ is defined as the distance from the rotation axis of the output shaft (*O*) to the center of the slider (*B*). In this paper, the variation of ρ is presumed to be a cosine function, which has the expression as follows:

$$\rho = a + b\cos(N\theta_0), \tag{1}$$

where θ_0 is the angular position of the output shaft (*OB*), *a* and *b* are two arbitrary constants, and *a* must bigger than *b* for $\rho > 0$. The minimum of ρ is equal to (*a*-*b*), and the maximum is equal to (*a*+*b*), and the amplitude of variation is equal to 2*b*. Based on the length law of triangle, the maximum of ρ should be satisfied to two inequalities

$$\begin{cases} a+b<l_1+l_4 \\ a+b<l_2+l_3 \end{cases}. \tag{2}$$

Accordingly, coordinates of the slider (B_x and B_y) which traces a groove curve, can be expressed as:

$$\begin{cases} B_x = [a+b\cos(N\theta_0)]\cos(\theta_0) \\ B_y = [a+b\cos(N\theta_0)]\sin(\theta_0) \end{cases}. \tag{3}$$

Apparently, groove curves generated by Eq. (3) are a periodic function, and its period *T* is equal to

$$T = 2\pi / N. \tag{4}$$

Fig. 2(a) shows a groove curve with $N = 4$, and its period is equal to $\pi/2$. It means that as the output shaft rotates one revolution, the slider (*B*) will alternately move toward and then away from the center (*O*) four times.

As shown in Fig. 2(b), the angular positions of the two

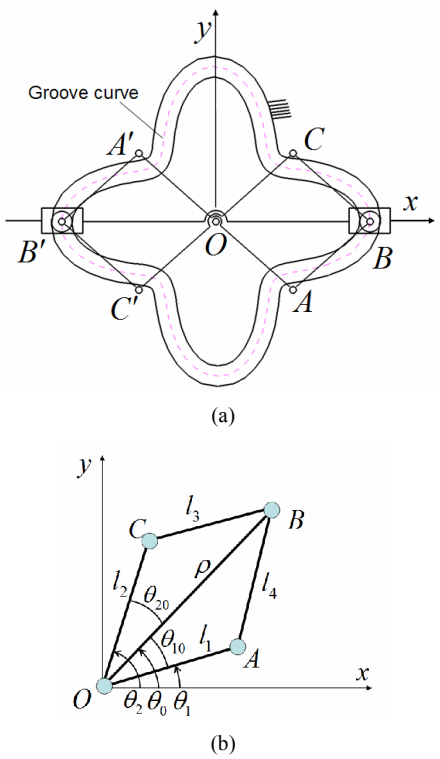

Fig. 2. Definitions of coordinates and angular position of kinematical modeling of TRPE: (a) initial position; (b) definitions of the angular positions.

rockers can be easily expressed as:

$$\begin{cases} \theta_1 = \theta_0 - \theta_{10} \\ \theta_2 = \theta_0 + \theta_{20} \end{cases} \tag{5}$$

where θ_{10} and θ_{20} are the relative angle between the respective rocker and the output rod, which can be deduced by law of cosines:

$$\begin{cases} \cos(\theta_{20}) = [(l_2)^2 + \rho^2 - (l_3)^2]/2l_2\rho \\ \cos(\theta_{10}) = [(l_1)^2 + \rho^2 - (l_4)^2]/2l_1\rho \end{cases}. \tag{6}$$

Assume the output shaft rotates at constant angular velocity, i.e., $\theta_0 = \omega_0 t$ (rad/sec), and $\alpha_0 = 0$. So the angular velocities of the two rockers (or the two rotors), ω_1 and ω_2, are obtained by differentiating Eq. (5) with respect to time, t, and can be expressed as:

$$\begin{cases} \omega_1 = \omega_0 - \omega_{10} \\ \omega_2 = \omega_0 + \omega_{20} \end{cases} \tag{7}$$

where ω_{10} and ω_{20} are derived by differentiating Eq. (6), and can be expressed as:

$$\begin{cases} \omega_{10} = \dfrac{\dot{\rho}(l_1 \cos\theta_{10} - \rho)}{l_1 \rho \sin\theta_{10}} \\ \omega_{20} = \dfrac{\dot{\rho}(l_2 \cos\theta_{20} - \rho)}{l_2 \rho \sin\theta_{20}} \end{cases} \tag{8}$$

where $\dot{\rho} = d\rho / dt = -bN\sin(N\theta_0)$.

Similarly, the angular accelerations of the two rockers (or the two rotors) α_1 and α_2, are obtained by differentiating Eq. (7) with respect to time, and can be expressed as:

$$\begin{aligned} \alpha_1 = \alpha_{10} &= \frac{\ddot{\rho}(l_1 \cos\theta_{10} - \rho)}{l_1 \rho \sin\theta_{10}} \\ &+ \frac{\dot{\rho}(\rho^2 \omega_{10} \cos\theta_{10} - l_1 \sin\theta_{10} \cos\theta_{10} - l_1 \rho \omega_{10})}{\rho^2 l_1 \sin^2(\theta_{10})} \\ \alpha_2 = \alpha_{20} &= \frac{\ddot{\rho}(l_2 \cos\theta_{20} - \rho)}{l_2 \rho \sin\theta_{20}} \\ &+ \frac{\dot{\rho}(\rho^2 \omega_{20} \cos\theta_{20} - l_2 \sin\theta_{20} \cos\theta_{20} - l_2 \rho \omega_{20})}{\rho^2 l_2 \sin^2(\theta_{20})} \end{aligned} \tag{9}$$

where $\ddot{\rho} = d^2\rho / d^2t = -bN^2 \cos(N\theta_0)$.

3.2 Power density of TRPE

The shape of the hypocycloidal curve is mostly determined by the parameters *N*. As shown in Fig. 3, there are many groove curves that can be applied as the trajectory of the slider. *N* is equal to the number of petals on the curves, and it also means that the slider (*B*) will alternately move toward and then away from the center (*O*) *N* times as the output shaft rotates one revolution. To sufficiently utilize the *N* oscillations and assure intake and exhaust ports positioned at a fixed angular relative to the housing, the number of vane pistons on each rotor should be equal to *N*. *N* may vary from two, the minimum number required to achieve a complete four-stroke cycle, to twelve, which is the maximum number that the rotor can accommodate, and is chosen based on the specific strength requirements, the adopted thermodynamic cycle, and other design considerations.

If the TRPE is adopted to be a spark ignition engine with four-stroke cycle, then *N* must be an even number, and the engine's configuration includes 2*N* vane pistons, 2*N* working chambers, *N*/2 ignition devices, *N*/2 intake ports, *N*/2 exhaust ports.

As one oscillation means a contraction and an expansion phases for each working chamber, thus in one revolution of the output shaft, each of 2*N* working chambers completes *N*/2 power strokes. Thus, the number of power strokes per revolution of the output shaft is equal to

$$C = N^2. \tag{10}$$

The respective ones of the four cycles are carried out simultaneously in each *N*/2 spaced working chambers. So TPRE mechanism also provides a balance of pressure forces within the 2*N* working chambers, and increases the power density of the engine due to multiple utilization of the working space of the housing.

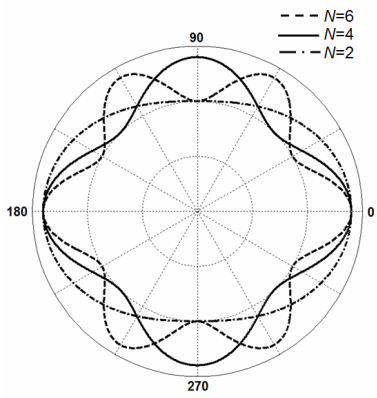

Fig. 3. Three sets of groove curves for the TRPE with *N* = 2, 4, and 6, respectively.

3.3 Compression ratio and engine displacement

As shown in Fig. 4, δ is the relative angle of the adjacent vane pistons, which can be expressed as:

$$\delta = \theta_Y - \theta_L - \beta \tag{11}$$

where β is the span angle of the vane pistons, θ_Y and θ_L are the angular positions of the rotors. It is a valid assumption that the vane pistons are identical and have the same β in this paper. So

$$\beta = \frac{2\pi - N(\delta_{\min} + \delta_{\max})}{2N} \tag{12}$$

where $\delta_{\max}$ and $\delta_{\min}$ are the maximum and minimum of δ.

The volume of working chamber Ⅰ, *V*, is proportional to δ

$$V = \frac{[(d_2)^2 - (d_1)^2]h\delta}{8} \tag{13}$$

where d_1 and d_2 are the diameter of the inner and outer wall of the working chamber, h is the depth of the working chamber in the axial direction.

Thus, it has an extreme with respect to time when

$$\frac{dV}{dt} = 0 \Leftrightarrow \frac{d\delta}{dt} = 0 \Leftrightarrow d\theta_Y = d\theta_L . \tag{14}$$

For a greater and more complete intake, it must start at the smallest value of the volume between two vane pistons and finish when this volume reaches the maximum value. The same statement is valid for all other regimes (intake, compres-

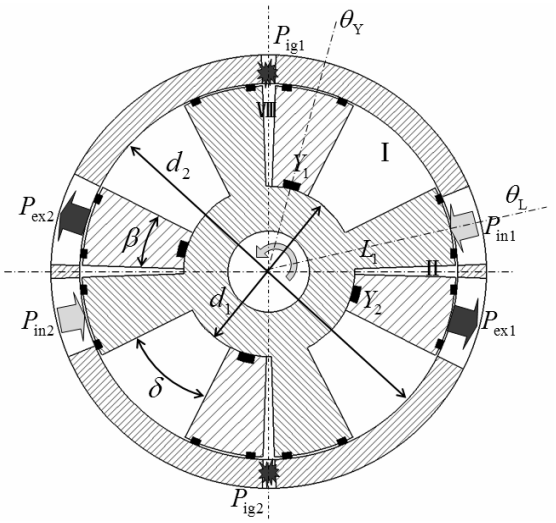

Fig. 4. ECS at $\theta_0 = \pi/4$.

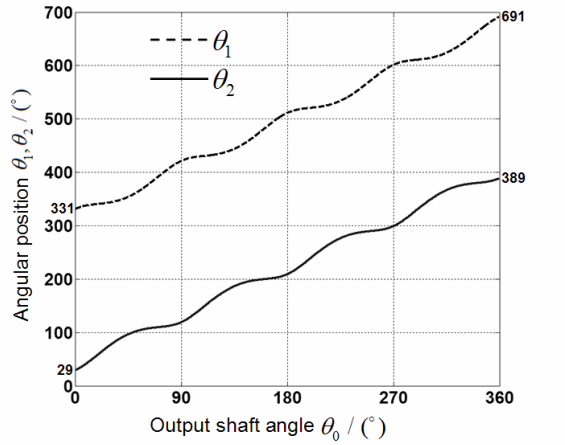

Fig. 5. Angular positions of the former and the latter rocker versus the output crankshaft angle.

sion, combustion, exhaust). Therefore, each regime must start and finish when $d\theta_Y = d\theta_L$, i.e., the two rotors have the same velocity when the working volume reaches its maximum or minimum.

Taking the working chamber Ⅰ for example, Fig. 1(a) shows the working chamber Ⅰ reaches its minimum at $\theta_0 = 0$; Fig. 4 shows the working volume Ⅰ reaches its maximum at $\theta_0 = \pi/4$. As each of the two rockers is fixed on a respective rotor, $d\theta_Y = d\theta_L$ also means $\omega_1 = \omega_2$, i.e., the two rockers have the same velocity when the working volume reaches its maximum or minimum. So as the output shaft rotates from 0 to $\pi/4$, the former rotor rotates an angle of $\beta + \delta_{max}$, and the latter rotor rotates an angle of $\beta + \delta_{min}$; it can be expressed as:

$$\begin{cases} \beta + \delta_{max} = \int_0^{\pi/4} \omega_1 d\theta_0 \\ \beta + \delta_{min} = \int_0^{\pi/4} \omega_2 d\theta_0 \end{cases}. \tag{15}$$

The two rotors rotate the above two angles alternately. With Eqs. (12) and (15), it is easily concluded that

$$\begin{cases} \int_0^{\pi/4} (\omega_1 - \omega_2) d\theta_0 = \delta_{max} - \delta_{min} \\ \int_0^{\pi/4} (\omega_1 + \omega_2) d\theta_0 = \dfrac{2\pi}{N} \end{cases}. \tag{16}$$

That means the variation of relative angle of the two rockers is equal to $\delta_{max} - \delta_{min}$, and the summation of the angles covered by the two rockers is always equal to $2\pi/N$. The phenomenon can also be seen in Table 1 below.

The compression ratio of the engine, ε, can be expressed as:

$$\varepsilon = \frac{V_{max}}{V_{min}} = \frac{\delta_{max}}{\delta_{min}}. \tag{17}$$

Similar to the displacement definition of the conventional piston engine[1], the displacement of the TRPE engine, Q_{ex}, is the gas volume exhausted from the 2N working chambers per revolution of the output shaft, which can be expressed as:

$$Q_{ex} = \frac{N(\pi - N\beta)[(d_2)^2 - (d_1)^2]h(\varepsilon - 1)}{4(\varepsilon + 1)}. \tag{18}$$

4. Kinematic analysis of the TRPE

For simplicity, it is valid to assume that the length parameters of the four components of the quadrilateral are identical, i.e., l_1=l_2=l_3=l_4=l. This assumption assures the TRPE is not only a balance but also a symmetry mechanism. However, the above kinematic modeling of TRPE establishes a more general situation considering optimization on manufacture, deformation, and transmitting power.

4.1 Position analysis of the TRPE

As an example, set N = 4, a = 120 mm, b = 20 mm, l = 40 mm to demonstrate the characteristics of the motion of TRPE. Substituting these parameters into Eqs. (5) and (6), the variation of the angle of all components can be obtained. Fig. 5 shows a plot of angular position of the former and the latter rocker, versus the output shaft angle. It will be noted that the angular position of the rockers (also the rotors) varies with a cyclic rotary motion superposed on uniform rotary motion. The motion of the two rockers has many similarities. On the one hand, the rockers rotate with the same pattern but at different paces, i.e., one rocker accelerates while the other rocker

Table 1. Comparison of angles at max/min relative angle of the two rockers.

Angular position (/ ◦)	θ_0	θ_1	θ_2
Initial position	0	331	29
The angles at min relative angle of the two rockers	90	421	119
	180	511	209
	270	601	299
The angles at max relative angle of the two rockers	45	354	96
	135	444	186
	225	534	276
	315	624	366
Final position	360	691	389

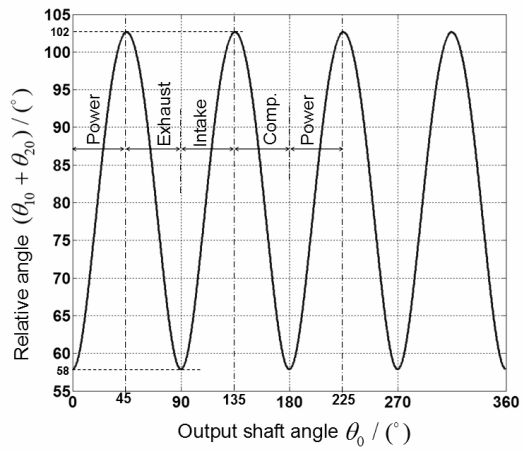

Fig. 6. The relative angle between the two rockers versus the output shaft angle.

decelerates. On the other hand, the rockers continuously rotate in the same direction, and one revolution of the rockers (one rotates from 29° to 389°, the other from 331° to 691°) is equivalent to one revolution of output crankshaft (from 0° to 360°).

Table 1 shows a comparison of angles at max/min relative angle of the two rockers. It can be seen that the variation of the output shaft angle between two adjacent max/min relative angle of the two rockers is equal to $2\pi/N$ (in this example N = 4, i.e. = 90°, similarly hereinafter), and the variation of the output shaft angle between the max and the min is π/N. In addition, in the output shaft's each rotation angle of π/N, the summation of the angles covered by the two rockers is always equal to $2\pi/N$. In this example, the two rockers rotate 23° or 67° alternately. Thus the summation is 90° and the difference is 44°. It also can be deduced that the variation of relative angle of the two rockers is equal to 44°.

As shown in Fig. 6, the variation of the relative angle of the two rockers has the period of $2\pi/N$.

Obviously, working chambers reach their maximum volume at the peak or valley of curves. At the peak of relative

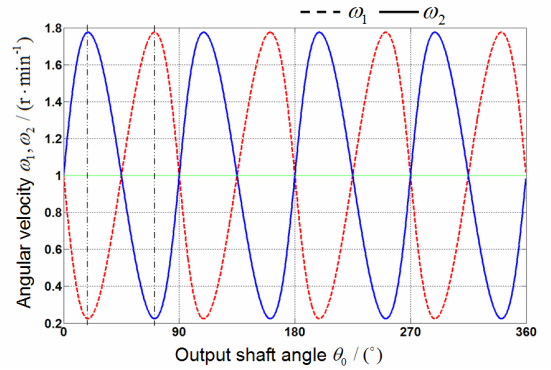

Fig. 7. Angular velocities of the former and the latter rocker versus the output crankshaft angle.

angle curve ($\theta_0 = 90°k$, k = 0,1,2, ⋯), the working chambers denoted by an odd number (Ⅰ, Ⅲ, Ⅴ, Ⅶ) are at the start of intake or power cycle, while other working chambers are at the end of intake or power cycle, and at the valley of the curve ($\theta_1 = 45°k$), the working chambers with an odd number are at the start of exhaust or compression while other working chambers are at the end of exhaust or compression.

4.2 Velocity analysis of the TRPE

The angular velocity of the rockers (or the respective rotors) can be obtained by assuming the angular velocity of the output shaft $\omega_1 = 1$ (r/min). As shown in Fig. 7, the rockers (or the rotors) alternately speed up and down, varying from maximum to minimum or from minimum to the maximum four times during one revolution of the output shaft. The rotational speed of each of the two rockers is a near sinusoidal motion. This periodic variation for the two rockers being out of phase causes the volume of each of the eight working chambers to alternately expand and reduce. Both of the two rockers have the same average speed and the same speed when the chamber volume reaches its minimum or maximum, which are equal to the speed of the output shaft.

4.3 Acceleration analysis of the TRPE

Assume $\omega_1 = 1$ (r/min) and α_1 =0, the angular acceleration of the two rockers (or the two respective rotors) is illustrated in Fig. 8. Unlike angular velocity, the two rockers exhibit different patterns of angular acceleration. However, the two curves are symmetrical about the zero acceleration line, so the maximum and minimum angular accelerations of two rockers occur at the same output shaft angles, i.e., when a rocker reaches its maximum angular acceleration, the other rocker reaches its minimum angular acceleration, and vice verse. As the angular acceleration is proportional to the inertial moment, so the inertial forces generated by the two oscillations of the rotors are also equal to zero. In addition, all components in TRPE are arranged symmetrically. Therefore, the TPRE is a totally balanced mechanism statically and dynamically.

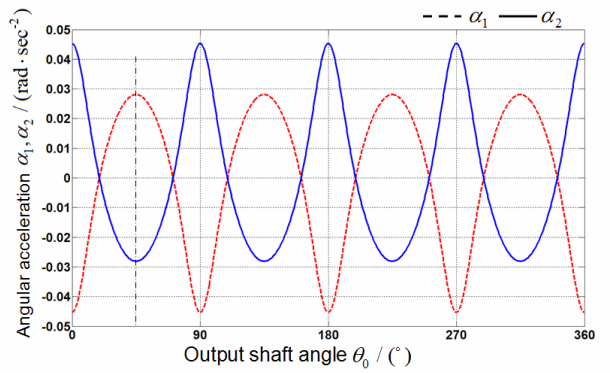

Fig. 8. Angular accelerations of the former and the latter rocker versus the output crankshaft angle.

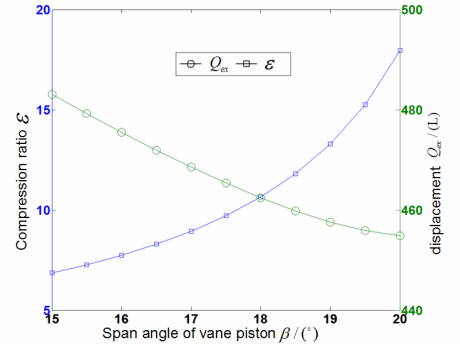

Fig. 9. Compression ratio and displacement of the engine versus span angle of vane piston.

4.4 Compression ratio and displacement of the TRPE

According to Eq. (16), the variation between the maximum and the minimum of relative angle of the two rockers ($\delta_{\max} - \delta_{\min}$) is determined by the given parameters of DVDM. Then, if the span angle of vane piston (β) is presumed as a known parameter, associated with Eqs. (15), (17) and (18), the compression ratio and displacement of the engine will be derived, which is shown in Fig. 12. In fact, on the one hand, the higher the value of the compression ratio, the higher the magnitude of the efficiency of the engine, On the other hand, Fig. 9 shows that the variation of compression ratio has the opposite direction to the variation of the displacement, which reflects the capability of output power of the engine when the span angle of vane piston increases. Assuming $d_2 = 300$ mm, $d_1 = 150$ mm, h = 80 mm, so with the above parameters, the span angle of vane piston β should be designed to be 18^0; accordingly, the compression ratio ε is 10.6, and the minimum of the relative angle of the adjacent vane pistons $\delta_{\min}$ is 4.6°, and the maximum $\delta_{\max}$ is 49.4°.

5. Statics analysis and experiment

The slide is the key part of TRPE which has the most complicated force condition such as: The link force (F) from the connecting rod, the contact force (F_{N1}) and the friction force (F_{f1}) between the slide and the output stick, the contact force (F_{N2}) and the friction force (F_{f2}) between the slide and the cam.

The forces would be different under each stroke. Taking the slide in the combustion stroke, for example, the forces of the slide undergone are shown in Fig. 10. Then, the balance equation is

$$\begin{cases} F_{N1} = F_{f2}\sin\alpha - F_{N2}\cos\alpha \\ -F_g + 2F\cos\theta_B = F_{N2}\sin\alpha + F_{f1} + F_{f2}\cos\alpha \end{cases} \tag{19}$$

where θ_B is defined as the relative angle between the rocker and the output stick. α is defined as the angle between the output stick and the tangency of the cam groove. Based on the definitions and Fig. 10, the two angles above can be expressed as:

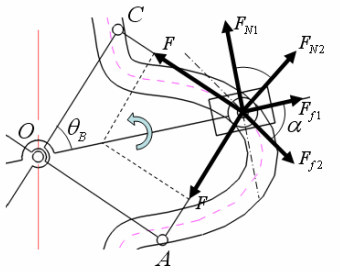

Fig. 10. Statics analysis of the slide in the combustion stroke.

$$\begin{cases} \theta_B = a\cos(\rho / 2l) \\ \alpha = \beta_t - \theta \end{cases} \tag{20}$$

where β_t is defined as the relative angle between the tangency of the cam groove and the output stick and the axis x shown in Fig. 2(a). So, with Eqs. (1) and (3), it can be calculated as

$$\tan\beta_t = \frac{\rho\cos\theta + \dot{\rho}\sin\theta}{-\rho\sin\theta + \dot{\rho}\cos\theta}. \tag{21}$$

Obviously, these above forces always exist: $F_{f2} = f_2 F_{N2}$, $F_{f1} = f_1 F_{N1}$, $F_g = m\rho\omega^2$, where m is the weight of the slide. For simplicity, F_g can be ignored as the speed of the slide is slow.

F is related to the output gas force which can be calculated in due course. F_{N1} is regarded as the output load. So

$$F_{N1} = \frac{2F\cos\theta_B}{f_\alpha + f_1} \tag{22}$$

where $f_\alpha = (\sin\alpha + f_2\cos\alpha)/(f_2\sin\alpha - \cos\alpha)$, when $\alpha = 0$, $f_\alpha = -f_2$, when $\alpha = 90^\circ$, $f_\alpha = 1/f_2$.

Set $F = 1000$ N, other parameters are set as shown in Sec.

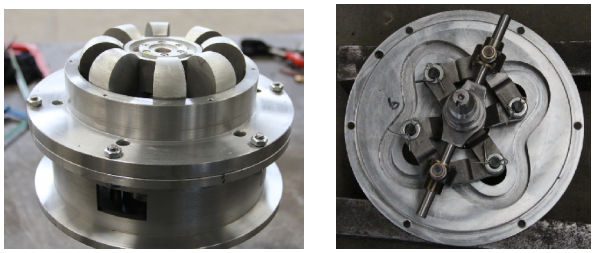

(a) (b)

Fig. 11. The prototype of TRPE: (a) engine assembly; (b) its DVDM.

4.1. Eq. (19) can be deduced. F_{N1} is equal to 1200N at the begin of the combustion stroke, then F_{N1} will increase to 1300N and then decrease. F_{N2} is equal to 200N at the start of the combustion stroke , it also will increase and then decrease. Thus the two contact forces is so big as the slider need to be designed with special structure and material.

To validate the working principle of TRPE, the prototype of TRPE is manufactured as shown in Fig. 11. It is compact and manufactured and assembled by module. Each rotor has four vane pistons. This engine has 16 power strokes per revolution of the output shaft. It works smoothly at a low speed. However, vibration of the engine is serious at a high speed over 1000 rpm. The main reason of vibration is probably the process preciseness of the cam.

6. Conclusions

The basic structure and working principles of TRPE were presented. The analysis results indicate that the TPRE engine performs the four−stroke cycle without using the valve mechanism, and reduces vibration noise due to totally balanced parts, and should be able to generate higher power density due to multiple utilization of work space and higher uniformity of torque due to multiple work strokes during one revolution. Furthermore, with this special cam−quadrilateral mechanism, the compression ratio of the TRPE engine may be easily adjusted by adjustment of the side length of quadrilateral, so it can also operate with optimum efficiency using a variety of fuels and atmospheric conditions.

The optimization of structure parameters requires further investigation, detailed consideration of hitherto sealing between the vane pistons of the rotors and the walls of the cylindrical housing, and thermodynamics analysis of the TRPE is also needed in the future.

Nomenclature

N : Number of vane pistons per rotor
T : Period
ρ : Length of diagonal of the quadrilateral
l_i : Length of side of the quadrilateral
θ_i : Angular position
ω_i : Angular velocity
α_i : Angular acceleration
B_x : X-coordinates of the slider
B_y : Y-coordinates of the slider
a, b : Arbitrary number
δ : Relative angle of the adjacent vane pistons
β : Span angle of the vane pistons
C : Number of power strokes per revolution
V : Volume of the working chamber
h : Depth of the working chamber
d_1 : Diameter of the inner wall
d_2 : Diameter of the outer wall
Q_{ex} : Engine displacement
θ_{10}, θ_{20} : Relative angle
ω_{10}, ω_{20} : Relative velocity
α_{10}, α_{20} : Relative acceleration
θ_Y, θ_L : Angular position of the rotors

References

[1] R. Stone, *Introduction to internal combustion engines*, 3rd ed. MacMillan, New York, USA (1999).
[2] M. J. Colaco, C. V. Teixeira and L. M. Dutra, Thermal analysis of a diesel engine operating with diesel-biodiesel blends, *Fuel*, 89 (12) (2010) 3742-3752.
[3] A. Kellaci et al., The effect of lubricant rheology on piston skirt/cylinder contact for an internal combustion engine, *Mechanika*, 1 (2010) 30-36.
[4] S. Manasijević, R. Radiša, Z. Aćimović-Pavlović and S. Marković i K. Raić; Thermal analysis and microscopic characterization of the piston alloy AlSi13Cu4Ni2Mg, *Intermetallics*, 19 (4) (2011) 486-492.
[5] S. Lee et al., Combustion and emission characteristics of HCNG in a constant volume chamber, *Journal of Mechanical Science and Technology*, 25 (2) (2011) 489-484.
[6] K. Nakashima et al., Behavior of piston rings passing over cylinder ports in two-stroke cycle engines, *Journal of Mechanical Science and Technology*, 24 (1) (2010) 227-230.
[7] J. Benajes, S. Molina, K. De Rudder and T. Rente, Influence of injection rate shaping on combustion and emissions for a medium duty diesel engine, *Journal of Mechanical Science and Technology*, 20 (9) (2006) 1436-1448.
[8] J. Karhula, Cardan gear mechanism versus slider-crank mechanism in pumps and engines, *Ph. D. Dissertation*, Lappeenranta University of Technology, Finland (2008).
[9] D. Ling, Z. Liang and X. Zhu. A preliminary inquiry into the problems of the power transmission mechanism for internal combustion engine, *Transactions of CSICE*, 8 (4) (2005) 301-313.
[10] H. G. Rosenkranz, CMC Scotch Yoke engine technology, *Ph. D. Dissertation*, Melbourne University, Victoria (1998).
[11] R. Mikalsen and A. P. Roskilly, A review of free-piston engine history and applications, *Applied Thermal Engineering*, 03 (15) (2007) 2339-2352.
[12] S. Ashley, A new spin on the rotary engine, *Mechanical Engineering*, 117 (4) (1995) 80-82.

[13] T. Korakianitis, Performance of a single nutating disk engine in the 2 to 500 kW power range, *Applied energy*, 86 (2009) 2213-2221.
[14] O. Nitulescu, Numerical simulation of the thermodynamics of a nutating engine, *Ph.D. Dissertation*, the University of Toledo, Toledo (2006).
[15] B. Hudson, The production of power by pure rotary means, *Ph.D. Dissertation*, RMIT University, Melbourne, Australia (2008).
[16] I. S. Ertesvag, Analysis of the vading concept-a new rotary-piston compressor, expander and engine principle, Proc. Of Institution of Mechanical Engineers, *Part A: J. of Power and Energy*, 216 (2002) 283-289.
[17] K.Yamamoto, *Rotary engine*, Sankaido Co., Ltd, Tokyo, Japan (1981).
[18] E. Kauertz, Rotary radial-piston machine, United States Patent, *US 3,144,007* (1967).
[19] B. Librovich, R. W. Tucker and C. Wang, On gear modeling in multisage rotary vane engines, *Meccanica*, 39 (2004) 47-61.
[20] B. Librovich, Analysis, design, and modeling of a rotary vane engines, Journal of Mechanical Engineering, ASME, 126 (2004) 711-718.
[21] M. et al., Theoretical study of differential velocity 4-vane pump, *Chinese Journal of Mechanical Engineering*, 38 (11) (2002) 66-70.
[22] M. Cheng et al., Study of eccentric circular-noncircular gears driving system of differential velocity vanes pump, *Chinese Journal of Mechanical Engineering*, 41 (3) (2005) 98-101.
[23] L. Liang, A rotary engine with two rotors and its design method, World Patent, *WO 2005/124122 A1* (2005).
[24] H. F. Chun, Alternative-step appliance rotary piston engine, United States Patent, *US 2004/0261758 A1* (2004).
[25] M. Sakita, A cat-and-mouse type rotary engine: engine design and performance evaluation, *Proc. Of the Institution of Mechanical Engineering, Part D: Journal of Automobile Engineering*, (220) (2006) 1139-1151.
[26] M. Sakita, Rotary piston engine, United States Patent, *US 6,446,595 B1* (2002).
[27] K. Mikio, Cat and mouse type rotary device utilizing grooves and rods for power conveyance, United States Patent, *US 2001/0046446 A1* (2001).
[28] J. O. Wieslaw, About a new concept of internal combustion engine construction I. rotary engines, *Proc. Of IMECE*, ASME, Boston, Massachusetts, USA, 66297 (2008).
[29] A. J. Shih, Kinematics of the cycloidal internal combustion engine mechanism, *Journal of Mechanical Design*, 115 (4) (1993) 953-959.
[30] H. Deng et al. A power transmission machine combined by cam and multi-rod mechanism, China patent, *ZL201120080599.6* (2011).
[31] C. Pan et al. A piston engine with annular connecting cylinders, China patent, *ZL201110331226.6* (2011).

Xiaojun Xu is currently an associate professor in the College of Mechatronics Engineering and Automation, National University of Defense Technology, China. His research interests include power generating machine design, new energy resource utilization, intelligent machine & digital design.